Enviromental Radioactivity

Gruppo n.12
Candiello Anita 1146534
Lonigro Nicola 1218058
Pergola Paolo 1238256

December 2019

Objectives

- Optimization of the energy resolution for both the HPGe detector and the NaI(Tl) detector adjusting the parameters of the trapezoidal filter;
- Calibration in energy and efficiency of the low background γ-ray detectors: NaI(Tl) and HPGe;
- Measurement of the radioactivity of a series of samples;
- Measurement of the quantity of Radon present in a room in the basement of the Polo Didattico.

Materials and Instrumentations

- Na-22 source
- Am-241 source
- Eu-152 source
- Radioactive samples
- NaI(Tl) scintillator detector
- HPGe detector
- CAEN power module
- CAEN digitizer DT5780
- Tektronix TBS 1012B-EDU Oscilloscope

Detector	V (mV)	Rise Time (ns)	Noise Level (mV)
NaI	750 ± 150	700 ± 100	64 ± 4
HPGe	$(3.28 \pm 0.5)10^3$	135.7 ± 11	3.16 ± 0.5

Table 1: Signal output from detectors for 511 keV photon

Detector	Threshold	DecayTime	Rise Time (ns)	FlatTop	Rescaling
NaI	15	8500	500	250	18
HPGe	400	4600	550	300	21

Table 2: Trapezoidal filter settings

Calibration of the detectors

A Na-22 source was initially used for the calibration of the detectors. The signals were analyzed using the oscilloscope, obtaining the results in Tab.1.

Having checked the characteristics of the signal, the outputs of the detectors were sent to the digitizer and using the calibration source the parameters of the trapezoidal filter were optimized to maximize the resolution of the apparatus (Tab.2).

The detectors were calibrated using the 511 keV and 1275keV peaks of the Na-22 and the 59.5 keV peak of the Am-241. A spectrum of 10 minutes was acquired for each source, put at a distance of $d_1 = 28.5 \pm 0.5$ cm from the NaI detector and $d_2 = 20.0 \pm 0.5$ cm from the HPGe detector. The peaks were fitted to obtain their positions in terms of the channels of the digitizer and the three data points were fitted to obtain the calibration line of the two detectors, as shown in Fig.1

Knowing the distance between the sources and the detectors and the activities of the sources it was possible to determine the efficiencies of the detectors. In particular knowing that the radius of the NaI scintillator is equal to $r_1 = (37.5 \pm 0.5)mm$ and the surface of the HPGe detector in equal to $s_1 = (1200 \pm 1)mm^2$, the fraction of solid angle covered by the detectors was estimated as

$$\Omega = \frac{S}{4\pi d^2}$$

where S is the surface of the detector and d the source-detector distance. The number of photon hitting a detector during a measurement of time t will then be given by

$$N_h = A \cdot F \cdot \Omega \cdot t$$

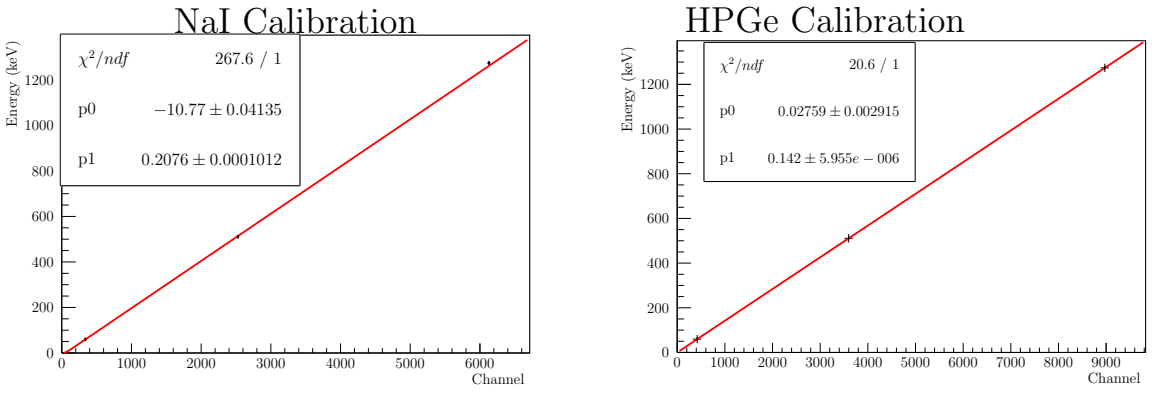

Figure 1: Calibration fit for the detectors

Peak Energy (keV)	**N(E)**	**A (kBq)**	**F**	**Efficiency**
NaI				$\Omega = (4.33 \pm 0.2)10^{-3} srad$
59	$(5.14 \pm 0.04)10^4$	408.0 ± 0.1	0.359	0.135 ± 0.006
511	$(9.1 \pm 0.2)10^3$	4.5 ± 0.1	1.8	0.43 ± 0.02
1275	$(1.93 \pm 0.09)10^3$	4.5 ± 0.1	0.99	0.162 ± 0.01
HPGe				$\Omega = (2.27 \pm 0.1)10^{-3} srad$
59	$(2.283 \pm 0.007)10^5$	408.0 ± 0.1	0.359	1.14 ± 0.06
511	$(1.82 \pm 0.07)10^3$	4.5 ± 0.1	1.8	0.164 ± 0.01
1275	$(4.6 \pm 0.4)10^2$	4.5 ± 0.1	0.99	0.075 ± 0.07

Table 3: Detector efficiency

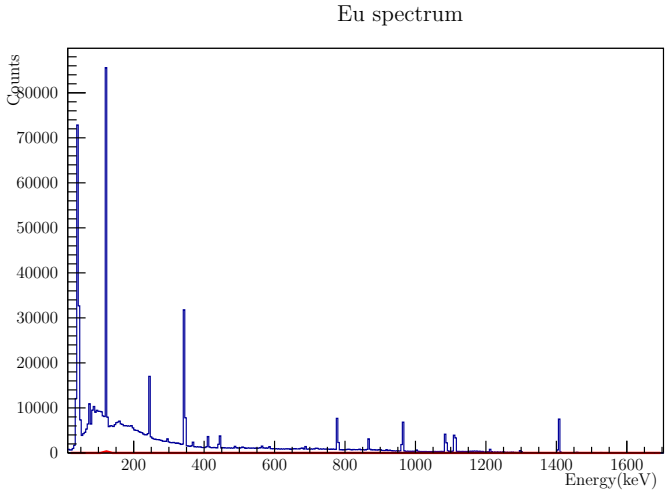

Figure 2: Eu-152 spectrum

where A is the activity of the sample and F a factor depending on the particular transition related to the gamma of that energy. The number of photon of a certain energy measured by the detectors can be estimated as the area of the gaussian fitting the peak, divided by the width of the bins after having removed the background. Using these relations is possible to estimate the efficiency of the detectors at a given energy as

$$\epsilon_E = \frac{N(E)}{N_h(E)}$$

where N(E) is the number off photon measured in a peak centered at energy E. In Tab.3 the values obtained for the three calibration peaks are reported.

The efficiencies are within expectations given the types of detectors with the exception of the 59 keV peak in the HPGe detector. Given a probable error in the acquisition of the data, that particular data point was not used in the determination of the absolute efficiency curve. A spectrum for the Eu-152 was acquired for 20 minutes(Fig.2). By normalizing the areas of the peaks to the area of the peak at 1408 keV and dividing each area by the relative intensity of that transition in respect to the one at 1408 keV (reported in the literature), it was possible to obtain a relative efficiency curve (Tab.4).

To determine the activity of a sample emitting gamma of arbitrary energy it is necessary to know the efficiency of the detector at that energy. To have an estimate of these quantities the absolute efficiencies of the NaI detector were fitted with a Landau function and the relative efficiency curve

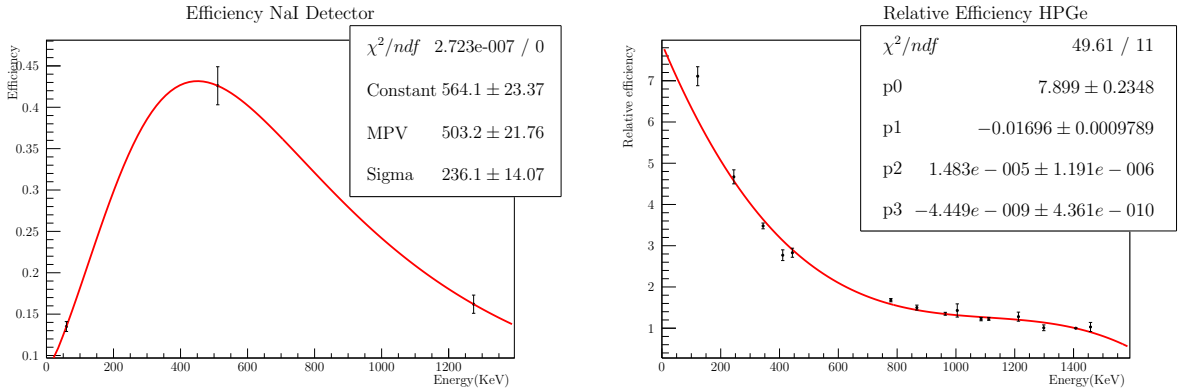

Figure 3: Efficiency interpolation

Peak Energy (keV)	122	245	344	411	444	779	867	964
Relative efficiency	7.1 ± 0.2	4.7 ± 0.2	3.48 ± 0.07	2.8 ± 0.1	2.8 ± 0.1	1.68 ± 0.04	1.50 ± 0.06	1.35 ± 0.04
Peak Energy (keV)	1005	1085	1112	1213	1299	1408	1457	
Relative efficiency	1.4 ± 0.2	1.22 ± 0.04	1.23 ± 0.04	1.3 ± 0.1	1.01 ± 0.07	1.00 ± 0.01	1.0 ± 0.1	

Table 4: HPGe relative efficiencies

of the HPGe was fitted with a polynomial of third degree. (Fig.3)

To obtain absolute values of efficiency for the HPGe detector the relative efficiency curve was rescaled to have efficiencies at 511 and 1275 keV equal to the ones obtained directly with the Na-22 source. In particular the mean of the two values obtained was taken giving a value of $S_f = 15 \pm 4$. During the second and third days the calibration procedure was repeated for the NaI detector, obtaining the calibration lines in Fig.4, while for the HPGe the calibration was checked and it was compatible with the one done during the first day.

Samples Radioactivity

In order to measure the activity of different radionuclides, the spectra of several samples were analyzed. For each gamma spectrum, measured with the HPGe detector and the NaI(Tl) detector, the area of the peaks was determined by using a gaussian fit and by substracting the appropriate background. The number of photons ($Counts$) of a certain energy detected by the detectors was measured as the area of the peak divided by the the width of the bins. The activity A_{sample} per

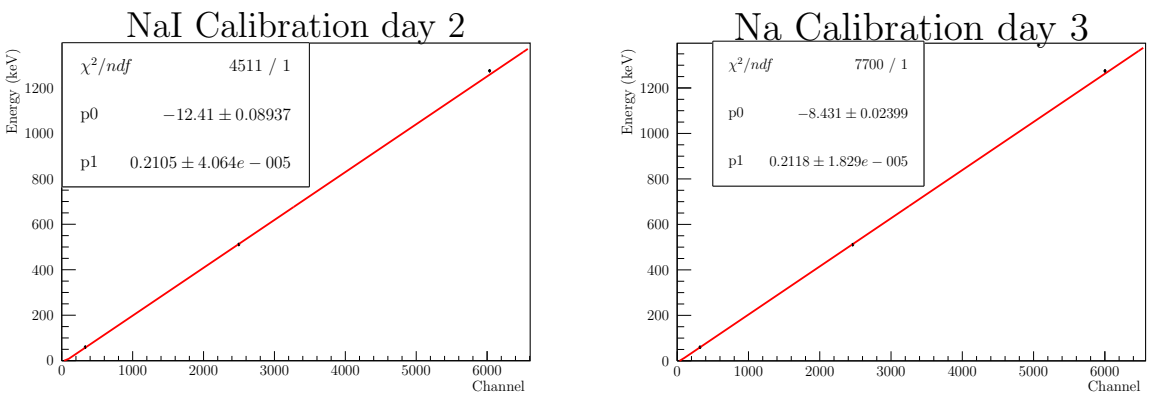

Figure 4: Calibration lines for the second (left) and third (right) day

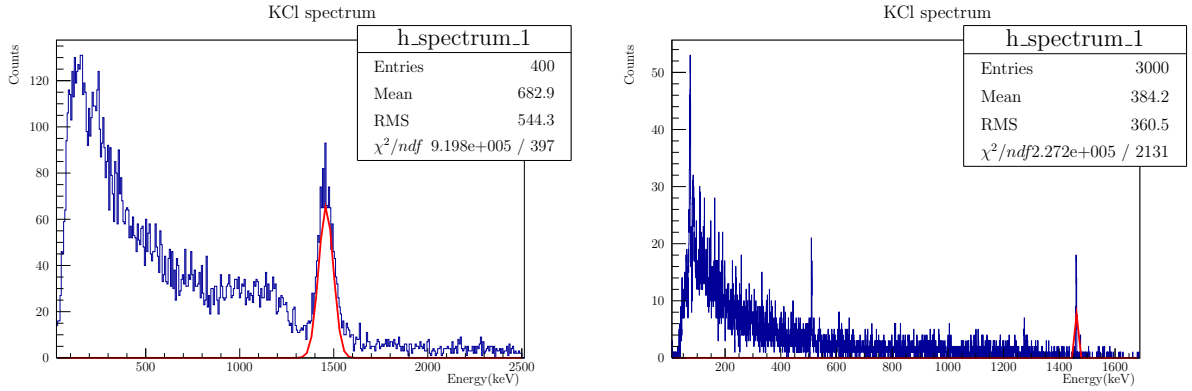

Figure 5: KCl spectra

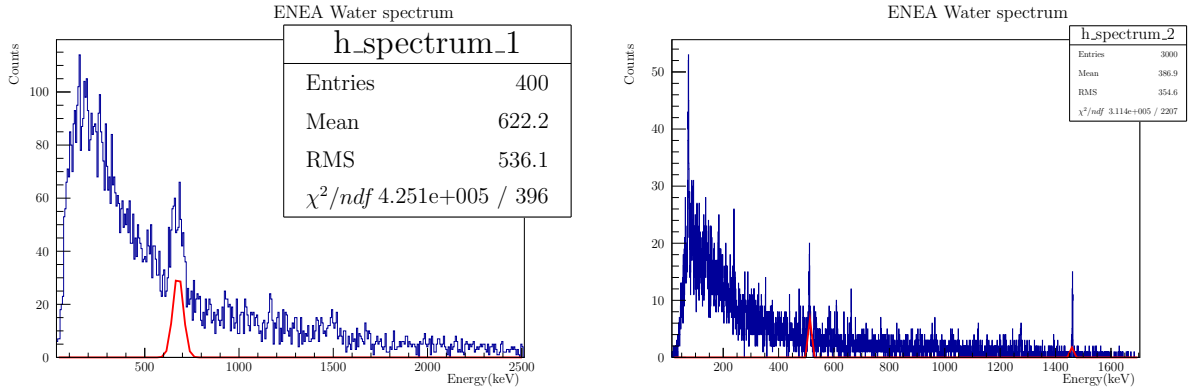

Figure 6: ENEA Certified water spectra

mass unit for a given sample and energy E was estimated by the following:

$$A_{sample}(E) = \frac{Counts}{\varepsilon(E) \cdot t \cdot \Omega \cdot F \cdot m}$$

where for the efficiency $\varepsilon(E)$ were used the functions determined in the first part with the parameters reported in Fig.3, t is the acquisition time, Ω is the solid angle fraction covered by the detectors, that results $\Omega = (0.9 \pm 0.4)$ for the NaI detector and $\Omega = (0.017 \pm 0.002)$ for HPGe considering a distance $d = (2.0 \pm 0.5)$cm and $d = (7.5 \pm 0.5)$cm respectively with respect to the sample and F is the value relative to the decay channel and present in literature. For the errors, the propagation of errors formula was used.

The calibration samples of KCl and ENEA certified water were analyzed first to check the correct use of the apparatus. In Fig.5 and Fig.6 the spectra of KCl and the ENEA certified water with both detectors are reported respectively, with the fit obtained after removing the background. The values of the fit are reported in Tab.5, along with the estimation of the activity.

The activity of the KCl sample (1.5 Bq/g) is underestimated with both detectors while the value obtained with the HPGe is compatible with the theoretical value, the same cannot be said for the NaI detector. This difference could be attributed to the fact that the efficiency curve of the NaI detector was obtained with only three data points and that the solid angle was difficult to determine, due to the dimension of the sample and it being very close to the detector. The activity obtained with the 673 keV peak of the NaI detector for the ENEA water sample strongly underestimates the correct value (0.0188 Bq/g) for the same reasons of the 1460 keV peak of the KCl, while the HPGe gives a reliable estimate of the activity of the sample with this peak.

Detector	Energy (keV)	Counts	Duration (min)	F	Activity (Bq/g)
KCL					
NaI	1459 ± 2	$(1.02 \pm 0.08)10^3$	30:15	0.10	0.04 ± 0.02
HPGe	1460 ± 0.2	83 ± 17	30:15	0.10	0.4 ± 1
Water					
NaI	674 ± 3	$(3.5 \pm 0.5)10^2$	30:05	0.849	$(1.4 \pm 0.7)10^{-3}$
HPGe	662.2 ± 0.2	28 ± 14	30:05	0.849	0.02 ± 0.01

Table 5: Calibration samples activity

For the selected samples, the mass m and the time t of the acquisition data for the spectra are reported:

- Zirconium Oxide, m=1870g, t=15.10min,
- mushrooms, $m = (51.20 \pm 0.02)$g, t=27.29min,
- porfido, $m = (536.80 \pm 0.02)$g, t=23.28min,
- brick from the ex-Military Base on Cansiglio, $m = (152.90 \pm 0.02)$g, t=17.18min.

The spectrum of the last sample was recorded the third day, while the others spectra were acquired the second day. Therefore the calibration considered for the NaI detector is different. The Table 6 shows the experimental values of the energy of the γ transitions found in the spectra, acquired with NaI and HPGe detectors, compared with the theoretical ones. The number of photon detected, the factor F and the activity of the radionuclides in Bq/Kg are also reported. In Table 7 the γ-rays are attributed to the father nucleus that decays into the nucleus son in an excited state and subsequently emits the studied γ.

Comparing the spectra acquired with the NaI detector to those acquired with the HPGe detector, it is visible that some peaks present in the spectra acquired with the first detector are missing in the second one. This is due to the lower efficiency of the Germanium detectors with respect to the NaI. To get a better statistic with HPGe detectors it is necessary to extend the time of measurement. Furthermore some peaks due to the low resolution of the NaI were identified only in one of the two detectors. Generally, the measured values of the activities are in a good agreement. The errors of the activities are high because the measurement of the solid angle is approximated. Indeed the distance between the detectors and the samples is not very precise since the samples have an extended volume, while they have been considered puntiform. In Figure 7 the analysed spectra of the samples are shown.

Radon Counting

In order to determine the activity of ^{222}Ra present in a room of the Polo Didattico building, in the first day a canister with activated charcoal was weighted and left open for two days in the room where the measurement was taken. The initial mass of the canister was:

$$m_i = (152.75 \pm 0.3)g$$

Part of the Radon gas present in the room was absorbed by the canister and the radioactive nuclides were caught by the canister: it was possible to determine the total Radon activity analyzing the

$E_{th}(keV)$	$F(\%)$	$E_{exp}^{NaI}(keV)$	Counts	A(Bq/Kg)	$E_{exp}^{HPGe}(keV)$	Counts	A(Bq/Kg)
Zirconium							
186.211	3.555	189.8 ± 0.4	8168 ± 498	535 ± 270	185.9 ± 0.1	1194 ± 94	220 ± 37
241.997	7.268	245.3 ± 0.3	16902 ± 621	453 ± 228	241.9 ± 0.1	716 ± 10	74 ± 16
295.224	18.414	299.3 ± 0.4	14028 ± 686	132 ± 67	295.2 ± 0.1	3063 ± 109	142 ± 24
351.932	35.60	362.2 ± 0.1	59566 ± 827	269 ± 134	351.9 ± 0.1	6148 ± 135	167 ± 31
609.312	45.49	621.9 ± 0.2	68029 ± 904	245 ± 123	609.2 ± 0.1	5433 ± 125	200 ± 40
768.356	4.892	790 ± 1	6296 ± 487	210 ± 107	768.2 ± 0.1	512 ± 51	226 ± 51
1120.287	14.91	1136 ± 1	10387 ± 560	212 ± 107	1120.0 ± 0.1	1359 ± 63	251 ± 551
1238.111	5.831				1238.0 ± 0.1	523 ± 43	261 ± 57
1377.669	3.968	1408 ± 2	4267 ± 445	277 ± 142	1378.0 ± 0.1	306 ± 36	254 ± 59
338.320	11.4				338.5 ± 0.1	295 ± 71	24 ± 7
911.196	26.2	951 ± 2	9794 ± 639	54 ± 27	911.0 ± 0.1	550 ± 47	52 ± 11
964.786	4.99				964.3 ± 0.2	89 ± 25	46 ± 16
968.96	15.9				969.0 ± 0.1	205 ± 30	33 ± 7
mushrooms							
661.659	84.99	684 ± 4	265 ± 59	11 ± 6			
porfido							
241.997	7.268	245.9 ± 0.7	1374 ± 120	8 ± 4	238.7 ± 0.1	119 ± 26	2.7 ± 0.7
295.224	18.414				295.8 ± 0.5	81 ± 34	0.8 ± 0.4
351.932	35.60	362 ± 2	545 ± 87	0.6 ± 0.3	352.2 ± 0.2	80 ± 18	0.5 ± 0.1
609.312	45.49	615 ± 2	856 ± 94	0.7 ± 0.4	609.4 ± 0.2	61 ± 13	0.5 ± 0.2
911.196	26.2	969 ± 4	501 ± 90	0.6 ± 0.3			
1460.822	10.55	1479 ± 3	1618 ± 158	19 ± 10	1461.0 ± 0.1	156 ± 21	13 ± 3
brick							
241.997	7.268	250 ± 3	159 ± 47	45 ± 26			
351.932	35.60	371 ± 1	207 ± 51	10 ± 6			
609.312	45.49	635 ± 4	172 ± 52	7 ± 4			
1460.822	10.55	1487 ± 5	244 ± 67	215 ± 123	1460.0 ± 0.2	30 ± 13	116 ± 56

Table 6: γ transition observed in the spectra acquired with the NaI and HPGe detectors for different samples and measured activities.

Nucleus	γ ray	Energy (keV)	**Nucleus**	γ ray	Energy (keV)
^{226}Ra	$\gamma(^{222}$Rn)	186.211	^{214}Pb	$\gamma(^{214}$Bi)	241.997
^{214}Pb	$\gamma(^{214}$Bi)	295.224	^{214}Pb	$\gamma(^{214}$Bi)	351.932
^{214}Bi	$\gamma(^{214}$Po)	609.312	^{214}Bi	$\gamma(^{214}$Po)	768.356
^{214}Bi	$\gamma(^{214}$Po)	1120.287	^{214}Bi	$\gamma(^{214}$Po)	1238.111
^{214}Bi	$\gamma(^{214}$Po)	1377.669	^{228}Ac	$\gamma(^{228}$Th)	338.320
^{228}Ac	$\gamma(^{228}$Th)	911.196	^{228}Ac	$\gamma(^{228}$Th)	964.786
^{228}Ac	$\gamma(^{228}$Th)	968.96	^{40}K	$\gamma(^{40}$Ar)	1460.822
^{137}Cs	$\gamma(^{137}$Ba)	661.659			

Table 7: Radionuclides and emitted γ-transitions

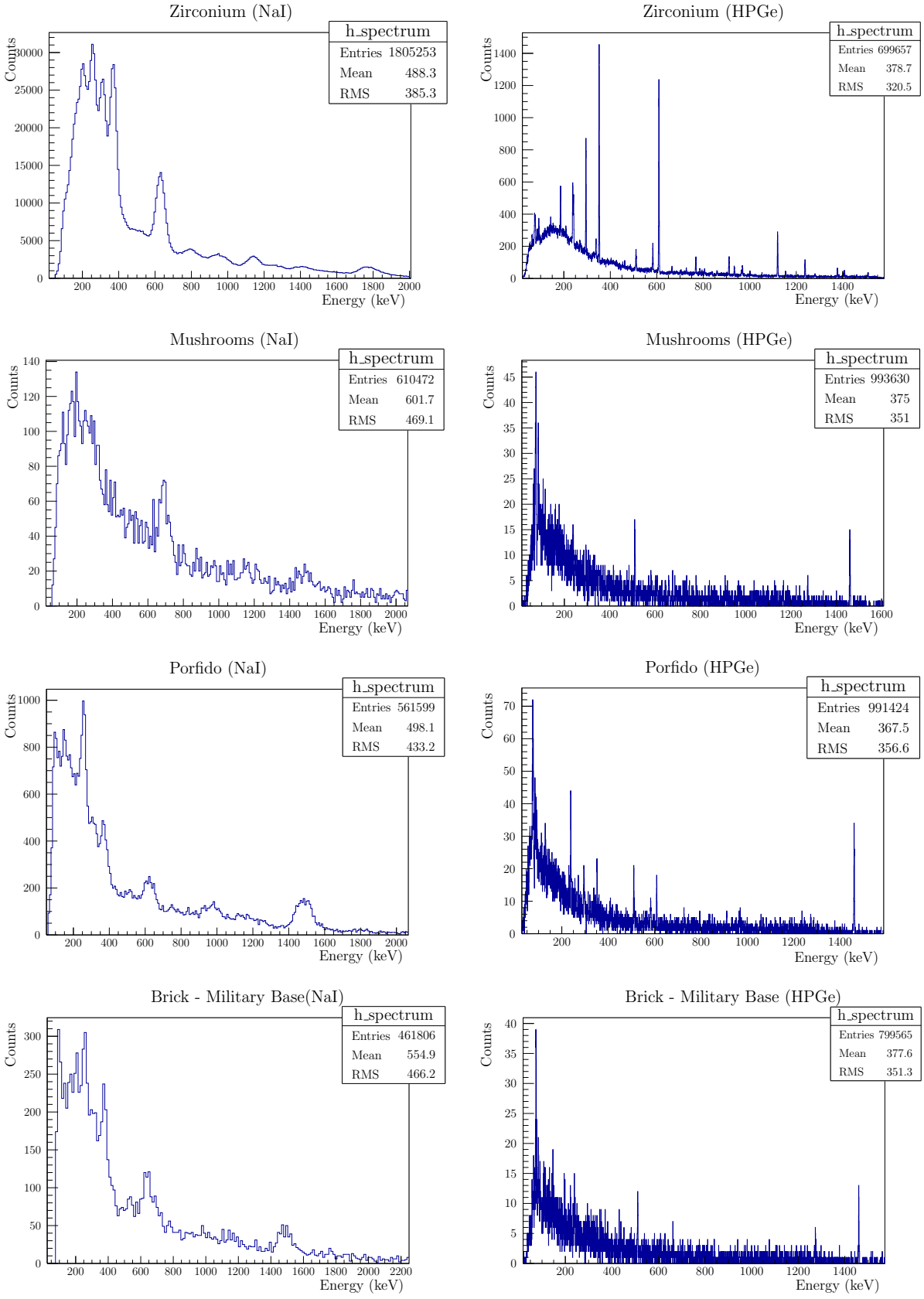

Figure 7: Spectra acquired with the NaI(Tl) detector and the HPGe detector for the samples: zirconium oxide, mushrooms, porfido, brick of a military base.

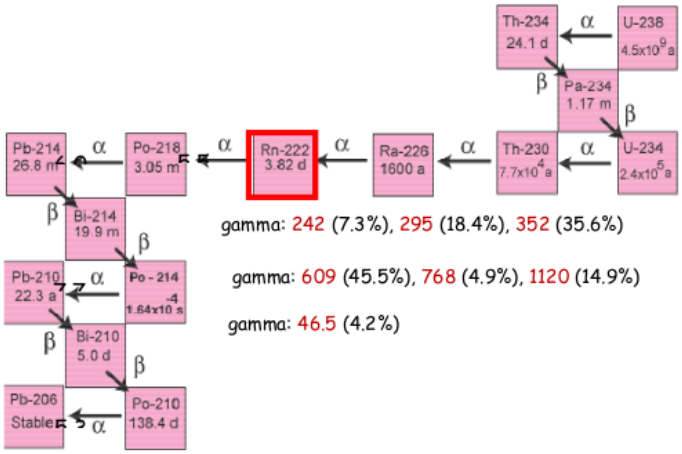

Figure 8: ^{222}Ra decay chain with the principal γ transitions and their branching ratios.

gamma transitions in the decay nuclei produced in the chain originating from ^{222}Ra, reported in Fig8, using both the NaI(Tl) detector and the HPGe detector. The calculation of Radon's activity per liter of air was done following the EPA's standard (Environmental Protection Agency - USA). At the beginning of the third day the canister was retrieved and sealed with the original adhesive tape. Weighting the removed canister it was obtained the value:

$$m_f = (159.10 \pm 0.02)g$$

The increase in weight $\Delta m = (6.35 \pm 0.04)$ g is due to the absorption of water vapour and from this value it was possible to determine the average humidity during the exposure, which in the case of a water gain greater than 4.0 g is fixed at 80%. These values are used to determine the calibration factor CF (in L/min) and the moisture dependent "adjustment" factor AF (in L/min), considering a total exposure time of $T_s = 2874$ min and the graphs of CF in function of the water gain and of AF in function of T_s present in the notes:

$$CF = (0.095 \pm 0.005)L/min \qquad AF = (0.090 \pm 0.005)L/min$$

which are already normalized for a time of exposure of 48 hours. The parameter CF indicates how many liters of air are presumably filtered per minute from the canister during the exposure. After having checked the calibration for both the detectors, the spectrum of a calibrated canister of known activity (^{226}Ra with $A = 14300$ pCi $\equiv 530$ Bq, measured in 27/1/1992)with mass $m_c = (178.10 \pm 0.02)$g was acquired for 30 minutes. Then the spectrum of the exposed canister was acquired for 30 minutes and finally it was acquired a background spectrum from a non-exposed canister. The spectra of calibrated and exposed canister with subtracted background for both the detectors are reported in Fig.9 and Fig.10.

From the spectra obtained by the NaI(Tl) detector it was possible to define an area of interest in energy for the analysis of the spectra in which there are all the principal γ-transitions of the Radon-chain. In our case it was selected a range of $[40; 1120]$keV in which all the transitions reported in Tab.8 and Tab.9 are included. Following the method applied for the analysis of the activity of the radioactive samples in the previous section, the different peaks in the spectra from the HPGe were fitted with gaussian functions compound with linear background, taking into account the Compton continuum at low energy. The results obtained for the activity of the single transitions for both the canisters are reported in Tab.8 and Tab.9. In the case of the calibrated canister it was also possible to determine the transition (^{226}Ra)$\gamma_{1,0}$ (^{222}Rn) at 186.1 keV.

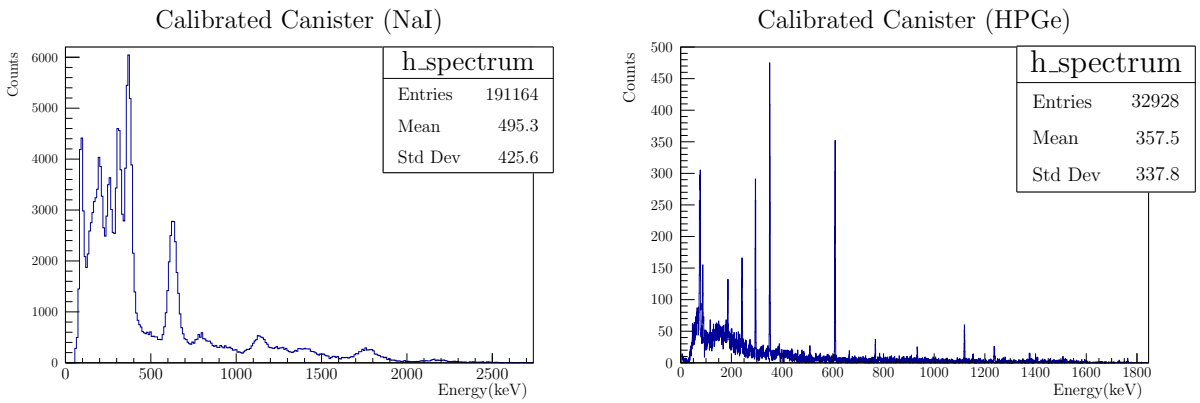

Figure 9: Calibrated canister spectra with background subtracted from the NaI(Tl) detector (left) and the HPGe detector (right).

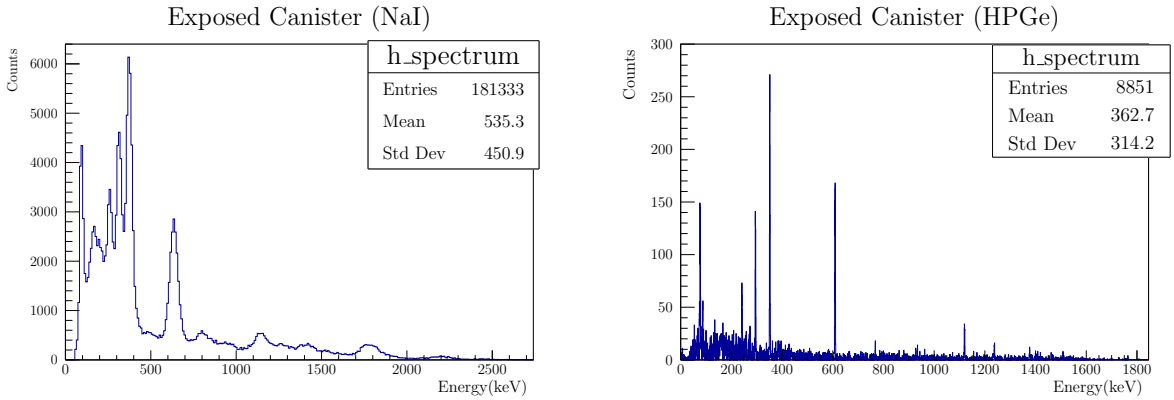

Figure 10: Exposed canister spectra with background subtracted from the NaI(Tl) detector (left) and the HPGe detector (right).

Transition	Energy (keV)	Counts/30min	F	Activity (Bq/kg)
$(^{214}\text{Pb})\gamma_{4,1}(^{214}\text{Bi})$	241.9 ± 0.1	481 ± 22	7.3%	83 ± 19
$(^{214}\text{Pb})\gamma_{4,0}(^{214}\text{Bi})$	295.0 ± 0.1	674 ± 26	18.4%	52 ± 10
$(^{214}\text{Pb})\gamma_{5,0}(^{214}\text{Bi})$	351.7 ± 0.1	1218 ± 35	35.6%	55 ± 12
$(^{214}\text{Bi})\gamma_{1,0}(^{214}\text{Po})$	609.0 ± 0.1	605 ± 25	45.5%	37 ± 7
$(^{214}\text{Bi})\gamma_{4,1}(^{214}\text{Po})$	768.1 ± 0.2	69 ± 8	4.9%	51 ± 13
$(^{214}\text{Bi})\gamma_{9,1}(^{214}\text{Po})$	1120.0 ± 0.1	128 ± 11	14.9%	39 ± 9

Table 8: Exposed canister activity calculated from each transition determined in the range of interest $[40; 1120]$keV. In this case F indicates the branching ratios for the transition.

Transition	Energy (keV)	Counts/30min	F	Activity (Bq/kg)
$(^{210}\text{Pb})\gamma_{1,0}(^{210}\text{Bi})$	46.58 ± 0.13	146 ± 12	4.2%	35 ± 4
$(^{226}\text{Ra})\gamma_{1,0}(^{222}\text{Rn})$	186.1 ± 0.1	435 ± 21	3.5%	124 ± 16
$(^{214}\text{Pb})\gamma_{4,1}(^{214}\text{Bi})$	241.9 ± 0.1	751 ± 27	7.3%	116 ± 19
$(^{214}\text{Pb})\gamma_{4,0}(^{214}\text{Bi})$	295.0 ± 0.1	1344 ± 37	18.4%	93 ± 16
$(^{214}\text{Pb})\gamma_{5,0}(^{214}\text{Bi})$	351.7 ± 0.1	1732 ± 42	35.6%	70 ± 15
$(^{214}\text{Bi})\gamma_{1,0}(^{214}\text{Po})$	609.0 ± 0.1	1346 ± 37	45.5%	73 ± 13
$(^{214}\text{Bi})\gamma_{4,1}(^{214}\text{Po})$	768.0 ± 0.1	75 ± 9	4.9%	49 ± 12
$(^{214}\text{Bi})\gamma_{9,1}(^{214}\text{Po})$	1120.0 ± 0.1	210 ± 15	14.9%	56 ± 13

Table 9: Calibrated canister activity calculated from each transition determined in the range of interest $[40; 1120]$keV. In this case F indicates the branching ratios for the transition.

In order to determine the overall Radon activity per liter of air RN from the exposed canister the following equation was used:

$$RN = \frac{N}{E \cdot T_s \cdot CF \cdot DF}$$

where E is the net number of counts per week of the calibrated canister in the region of interest (summing up the counts of all the transitions generated from Radon chain), divided by the known activity $A_{cal} = 14300$ pCi, N is the net number of counts per week for the exposed canister, DF is the decay factor which takes into account that part of the trapped Radon in the canister can decay before being counted, it was estimated as:

$$DF = exp^{(-(0.693t)/(5501)}$$

where t is the time in minutes from half of the exposure period of the canister to when its activity is measured. In our case it was $t = 1467$ and $DF = 0.831 \pm 0.008$. Summing up all the transitions in the region of interest it was obtained: $E = (132 \pm 4)$ Counts/(week$\cdot$ pCi), $N = (107 \pm 4) \cdot 10^4$ Counts/week. The final value of RN was then (with an error given by propagation):

$$RN = (36 \pm 5) pCi/L \equiv (1.33 \pm 0.19) Bq/L$$

The value obtained is well beyond the legal limit in working environments, which is 0.5Bq/L, in this case however it must be taken into account that the room in which the measurement was executed is small, poorly ventilated and in the basement of the Polo Didattico building so that this significant value for the activity can be justified considering an high concentration of Radon.

For the analysis of the Radon activity it may be interesting to consider a sample of Autunite, which is a radioactive mineral composed by Uranium. After having weighted the sample present in the laboratory, obtaining $m_s = (75.30 \pm 0.02)$g, the spectra of the Autunite from the NaI(Tl) detector and the HPGe detector were acquired (they are reported in Fig.11).

As in the case of the Radon activity determined from the canister, the NaI(Tl) spectrum was used to define a fixed energy window $[40; 1120]$keV where the analysis with the data acquired from the HPGe detector was executed. Following the procedure applied in the analysis of the radioactive samples in the previous section, the activity from the main γ transitions were determined. The results for the activity are reported in Tab.10.

The total activity of the sample can be determined considering the average value of the activity obtained from the γ transitions in Tab.10, obtaining the result:

$$A_{autunite} = (337 \pm 61) Bq/Kg$$

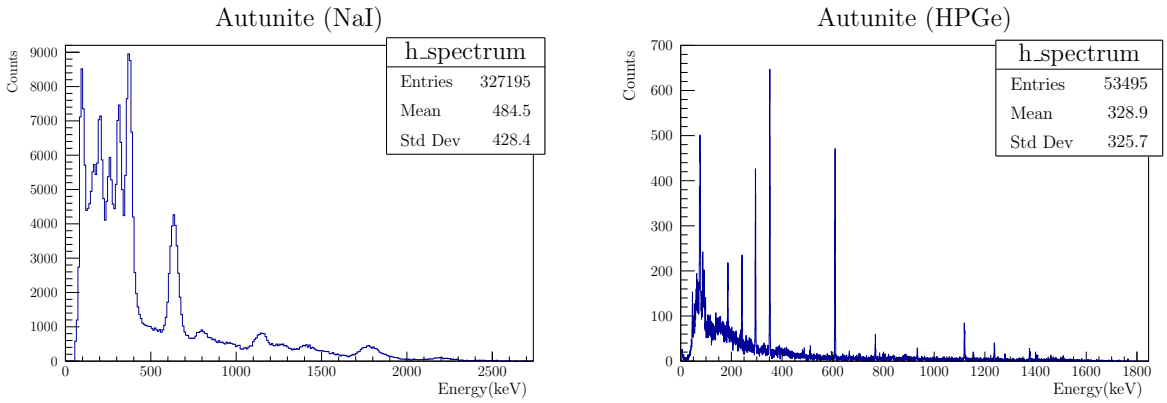

Figure 11: Autunite spectra with background subtracted from the NaI(Tl) detector (left) and the HPGe detector (right).

Transition	Energy (keV)	Counts/30min	F	Activity (Bq/kg)
$(^{210}\mathrm{Pb})\gamma_{1,0}(^{210}\mathrm{Bi})$	46.26 ± 0.09	945 ± 31	4.2%	390 ± 31
$(^{226}\mathrm{Ra})\gamma_{1,0}(^{222}\mathrm{Rn})$	186.0 ± 0.1	767 ± 28	3.5%	520 ± 71
$(^{214}\mathrm{Pb})\gamma_{4,1}(^{214}\mathrm{Bi})$	241.9 ± 0.1	686 ± 26	7.3%	252 ± 43
$(^{214}\mathrm{Pb})\gamma_{4,0}(^{214}\mathrm{Bi})$	295.1 ± 0.1	1584 ± 40	18.4%	259 ± 45
$(^{214}\mathrm{Pb})\gamma_{5,0}(^{214}\mathrm{Bi})$	351.8 ± 0.1	1928 ± 44	35.6%	186 ± 41
$(^{214}\mathrm{Bi})\gamma_{1,0}(^{214}\mathrm{Po})$	609.0 ± 0.1	2036 ± 45	45.5%	263 ± 45
$(^{214}\mathrm{Bi})\gamma_{4,1}(^{214}\mathrm{Po})$	768.0 ± 0.1	201 ± 14	4.9%	317 ± 63
$(^{214}\mathrm{Bi})\gamma_{9,1}(^{214}\mathrm{Po})$	1120.0 ± 0.1	369 ± 19	14.9%	235 ± 49

Table 10: Autunite activity calculated from each transition determined in the range of interest $[40; 1120]$keV. In this case F indicates the branching ratios for the transition.

Conclusions

During the laboratory experience the best possible resolution for the HPGe and NaI(Tl) detectors was obtained adjusting the parameters of the trapezoidal filter (decay time, rise time, flattop). The calibration in energy and efficiency of the detectors was then performed: it was possible to determine the intrinsic efficiency of the NaI(Tl) detector in terms of the energy considering a fit with a Landau function and the relative efficiency of the HPGe detector in terms of the energy considering a polynomial of third degree. Knowing the efficiencies of the detectors, the radioactive samples present in the laboratory were analyzed to individuate the γ transitions and to determine the activity of each radionuclide. Finally an indoor radon measurement was executed for a room of the Polo didattico building using the EPA's standard. The result obtained for the total activity is well beyond the legal limit for a working environment but this can be explained considering the fact that the room where the measurement was carried out was small and poorly ventilated so that there was an high concentration of Radon per liter of air. At last the Autunite sample was analyzed and the activity was determined.